Continental Shelf Research 54 (2013) 52–66

Contents lists available at SciVerse ScienceDirect

Continental Shelf Research

journal homepage: www.elsevier.com/locate/csr

Research papers

# Cold front induced changes on the Florida panhandle shelf during October 2008

D. Kamykowski [a,*], K. Grabowski Pridgen [b], J.M. Morrison [c], A.A. McCulloch [d], E.S. Nyadjro [e], C.A. Thomas [a], G.A. Sinclair [f]

[a] Marine, Earth & Atmospheric Sciences, North Carolina State University, Raleigh, NC, USA
[b] Naval Oceanographic Office, Stennis Space Center MS, USA
[c] Center for Marine Science, University of North Carolina at Wilmington, Wilmington, NC, USA
[d] Hatfield Marine Science Center, Oregon State University, Newport, OR 97365, USA
[e] Department of Earth and Ocean Sciences, University of South Carolina, Columbia, SC 29208, USA
[f] Defelice Center, Louisiana Universities Marine Consortium, Chauvin, LA 70344, USA

ARTICLE INFO

*Article history:*
Received 1 December 2011
Received in revised form
17 September 2012
Accepted 18 December 2012
Available online 16 January 2013

*Keywords:*
Karenia brevis
Pycnocline erosion
Winter mixing
Hydrographic transition
Pigment taxonomy
Gulf of Mexico

ABSTRACT

A significant step transition between seasonally stratified and destratified hydrographic conditions occurred during an October 2008 cruise to the Florida Panhandle Shelf along a cross-shelf transect that was sampled before and after a cold front passed through the area. Meteorological measurements from nearby ocean and land-based stations characterized the event. Cross-shelf continuous Acrobat profiles and discrete CTD stations characterized water column hydrographic patterns, while mid-shelf multicorer and box corer samples characterized sediment texture and nutrients. Water samples collected from selected depths biased toward the sediment interface were analyzed for nutrient content and phytoplankton community composition. Pre-front, the cross-shelf water column exhibited vertical stratification with complex temperature and salinity patterns. A prominent near-bottom chlorophyll *a* maximum of $\sim$1.5 μg $L^{-1}$ between the 25–35 m isobaths occurred with the 1% light level at $\sim$18 m depth and a near-bottom nitrate+nitrite ($NO_3^- + NO_2^-$) maximum $>$3 μM between the 30–40 m isobaths. HPLC-determined phytoplankton community composition in the near-bottom chlorophyll *a* maximum consisted of gyroxanthin-containing dinoflagellates (*Karenia brevis*) and less abundant diatoms, both verified by FlowCAM analysis, mixed with detectable cryptophytes and chlorophytes. Sediment trends based on limited core replicates suggested the sediments were a potential source of nutrients to near-bottom populations of *K. brevis* and that shell hash could provide abundant pore space for *K. brevis* incursions. Between the 40–50 m isobaths, diatoms, cryptophytes and chlorophytes dominated near-bottom, gyroxanthin-containing dinoflagellates and prasinophytes occurred throughout the water column, and cyanophytes dominated near-surface. Post-front, the cross-shelf water column exhibited destratification with temperature and salinity increasing offshore. A chlorophyll *a* maximum of $\sim$0.75 μg Chl *a* $L^{-1}$ left the sediment between 25–35 m isobaths and extended offshore especially in the lower water column with the 1% light level at $\sim$15 m depth and $NO_3^- + NO_2^-$ concentrations $\sim$2 μM to the 60 m isobath. HPLC-determined phytoplankton community composition of the offshore plume retained the signature of gyroxanthin-containing dinoflagellates and chlorophytes. Between the 30–50 m isobaths, prasinophytes increased in the lower water column, while cyanophytes increased at all depths across the shelf. The observed step transition from stratification to destratification on the Florida Panhandle Shelf contributed to altered phytoplankton community patterns in response to predominant downwelling favorable winds. Pre-front, *K. brevis* cells were broadly distributed cross-shelf, but concentrated near-bottom between the 25–35 m isobaths and staged for prolific bloom seeding in response to the upwelling favorable west winds more typical of spring-summer. Post-front, *K. brevis* cells were mixed throughout the mid-shelf water column and were staged for diffuse bloom seeding in response to either the downwelling or upwelling favorable winds occurring fall-winter. Cyanophytes located predominantly near-surface offshore pre-front, were ubiquitous cross-shelf and more closely associated with *K. brevis* post-front.



* Corresponding author. Tel.: +1 919 515 7894.
*E-mail address:* dkamyko@ncsu.edu (D. Kamykowski).

0278-4343/$ - see front matter © 2013 Elsevier Ltd. All rights reserved.
http://dx.doi.org/10.1016/j.csr.2012.12.006

## 1. Introduction

A destratified winter regime and the stratified summer regime occur on several wide, midlatitude continental shelves (Morey and O'Brien, 2002). One notable, well-studied US example is the Middle Atlantic Bight (Chapman and Gawarkiewicz, 1993). The West Florida Shelf (WFS) shows similar seasonal states (Weisberg et al., 1996; Liu et al., 2006) with a destratified regime from October to March and a stratified regime from April to September (Yang and Weisberg, 1999). During the winter, the water column is destratified due to both convective mixing as a result of cooling surface temperatures related to lower incident solar radiation and wind-induced mixing of the water column in response to frequent storms (He and Weisberg, 2001; Walsh et al., 2003). Colder, lower salinity water often is found near-shore due to the influence of enhanced riverine output, while warmer, higher-salinity water often is found on the outer-shelf influenced by the Loop Current (He and Weisberg, 2001). During the summer, warming sea surface temperatures due to higher incident solar radiation along with less frequent storms contribute to stratification (Walsh et al., 2003, He and Weisberg, 2003). Water column stratification results in increased lower water column nitrate+nitrite ($NO_3^- + NO_2^-$) that contributes to diatom (shallower) or dinoflagellate (deeper) dominated chlorophyll *a* concentrations depending on available light (Walsh et al., 2003). This seasonal hydrographic shift is accompanied by current direction changes as the net surface heat flux reverses the density gradient from seaward to landward (Weisberg et al., 1996).

The Florida Panhandle Shelf (FPS) is that part of the WFS bound to the east by Cape San Blas and to the west by the DeSoto Canyon. In contrast to the peninsular WFS, the FPS extends more east–west versus north–south, is narrower, and slopes more steeply (He and Weisberg, 2003). As with the peninsular WFS, the onset of summer heating yields cross-shelf stratification, while decreasing incident solar radiation and increasing storms in the fall (tropical hurricanes and subtropical cyclones) gradually convert the water column back to the destratified winter condition (He and Weisberg, 2001,2003; Walsh et al., 2003). The primary source of variability on the FPS combines deep-ocean processes and local forcing (Smith and Jacobs, 2005). The resulting flow fields on the FPS are mostly eastward, especially during spring near the shelfbreak and on the eastern portion of the shelf, but vary significantly on both the seasonal and interannual time scales. West winds favor the incursion of Mississippi River water (Muller-Karger et al., 2000) on the FPS. Furthermore, based on the east-west coastal orientation, west winds more typical of summer (He and Weisberg, 2003) favor upwelling (Weisberg et al., 2000), while east winds more typical of the rest of the year (He and Weisberg, 2003) favor downwelling (Muller-Karger et al., 2000). A proximate anticyclonic eddy derived from the Loop Current can enhance upwelling in the presence of a west wind (Muller-Karger et al., 2000) or reduce downwelling in the presence of an east wind (He and Weisberg, 2003). Typically, the DeSoto Canyon region is not directly influenced by the Loop Current or Loop Current Eddies except on rare occasions when they occur sufficiently north (Wang et al., 2003).

The present study focuses on a step in the fall transition between stratification and destratification. Meteorological and hydrographic, before and after a cold front passed through the study area, and sediment conditions are reported from an October 2008 cruise to the FPS (Nyadjro, 2009; Grabowski, 2010). FPS phytoplankton community redistribution patterns that include seed populations for *Karenia brevis* bloom initiation (He and Weisberg, 2003; Janowitz and Kamykowski, 2006; Janowitz et al., 2008) are considered in the context of the changing cross-wind forcing and shelf hydrography.

## 2. Methods

Photosynthetically active radiation (PAR) measured at the Apalachicola National Estuarine Research Reserve (NERR) station (ANS; 29.79°N, 84.88°W) (Fig. 1) and air pressure, wind speed/direction, and water temperature measured at National Oceanographic and Atmospheric Administration (NOAA) Buoy NB 42039 (29.21°N, 88.21°W) (Fig. 1) set the broader meteorological context between 1–31 October 2008 and the cruise-specific wind speed/direction context between 15–22 October 2008. FPS (coastal angle

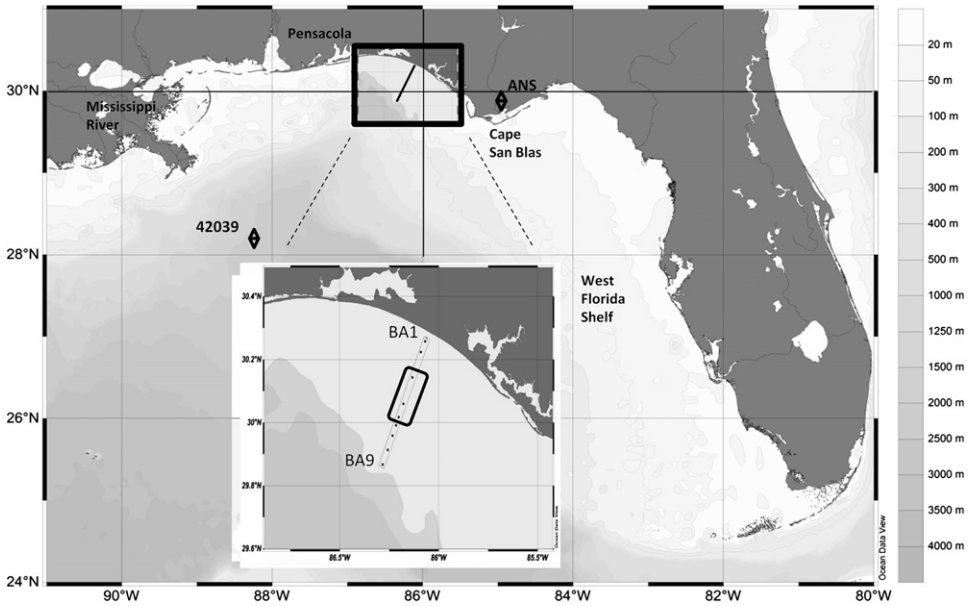


**Fig. 1.** Map of the Gulf of Mexico study area emphasizing the Florida panhandle shelf (FPS). The insert shows the transect (BA1 to BA9) that was repeatedly sampled between 15–21 October 2008 and the location of the coring effort mid-cruise (box) in the region of stations 3–5. Latitude 30°N and longitude 86°W are darkened for reference relative to the transect. The sites of the Apalachicola National Estuarine Research Reserve (NERR) station (ANS; 29.791°N, 84.883°W) and the NOAA Buoy (NB) 42039 (29.212°N 88.207°W) are also identified.

120° from Fig. 1) estimates of (1) the Global Upwelling Index (GUI; positive upwelling and negative downwelling) for all of 2008, but especially 1–31 October 2008, based on 6 h, 1° resolution sea surface pressure maps, and (2) transport vectors based on the application of Ekman theory for 16–21 October 2008 were obtained from the NOAA, Pacific Marine Environmental Laboratory, Southwest Fisheries Science Center Live Access Server (http://las.pfeg.noaa.gov/las6_5/servlets/dataset?catitem=1630).

The *R/V Pelican* staged from Pensacola, FL for a cruise 15–21 October 2008 to the FPS. The ship proceeded east to perform cross-shelf surveys between the 20–60 m isobaths along a repeated transect (Fig. 1) between 30.23° N, 85.08° W (BA1) and 29.87° N, 86.28° W (BA9) from 16–21 October 2008. On departure, the ship-based Multiple Instrument Data Acquisition System (MIDAS) recorded GPS navigational fixes, meteorological data, near-surface oceanographic data, and bottom depth. Based on predicted weather, the cruise was divided into pre-front and post-front efforts to account for passage of a cold front expected early (GMT) on 18 October 2008. The pre-front sequence included an undulating Acrobat survey on 16 October 2008 and an 8 station CTD/rosette survey (BA1–8) at 5 m intervals to the 55 m isobath on 17 October 2008. The post-front sequence included an undulating Acrobat survey followed by a 9 station CTD/rosette survey (BA1-9) at 5 m intervals to the 60 m isobath on 20 October 2008. Sediment core samples were collected near stations BA3 and BA5 (Fig. 1: black box in insert) between the pre-front and post-front efforts.

Underway SeaSciences Acrobat surveys with the instrument package undulating through the water column between the 25–60 m isobaths provided near-surface to near-bottom (5–10 m off bottom inside the 40 m isobath and 10–20 m off bottom beyond the 40 m isobath) surveys. Cross-shelf survey data reported here from 16–21 October 2008 were obtained using a SeaBird CTD package instrumented with SeaBird temperature, salinity, and dissolved oxygen sensors; SeaPoint chlorophyll and CDOM fluorescence and turbidity sensors; and a Brooke-Ocean Laser Optical Plankton Counter (LOPC) for plankton size spectra from 0.1 mm to 35 mm. At each hydrographic station, SeaBird CTD surveys provided profiles for light attenuation, pressure, temperature, salinity, dissolved oxygen, chlorophyll fluorescence and turbidity during the first downcast. Beam-*t* measurements obtained from the CTD transmissometer were used to approximate potential PAR attenuation based on the sequential application of the percent transmission through successive 1 m layers of the water column. A SeaBird Rosette on the CTD was configured with eleven 5 L Niskin bottles that were triggered during the first upcast near the sediment interface and then at 2 m intervals ($\sim$9 bottles) as well as mid-depth in the remaining water column to the surface (1 bottle) and at the surface (1 bottle). The seawater collected by the Rosette was used for nitrate–nitrite ($NO_3^- + NO_2^-$) analyses and HPLC pigment determinations. For $NO_3^- + NO_2^-$ samples (O'Dell, 1993), 10 ml of the filtered seawater were frozen immediately after collection and returned to NCSU for laboratory analyses. In the laboratory, these samples were thawed and analyzed against a standard of natural seawater with low nitrate concentrations. $NO_3^- + NO_2^-$ were determined colorimetrically at NCSU using an automated Quattro Continuous-Flow Analysis system (Grasshoff et al., 1983). Precision of the $NO_3^- + NO_2^-$ analysis was 0.1 μM with a detection limit of 1.4 μM.

For High-Performance Liquid Chromatography (HPLC) analysis (Jeffrey et al., 1997), approximately 1000 ml of water from selected sample depths were filtered through a 2.5 cm diameter GF-F filters under a low pressure vacuum ($<200$ mmHg). The filters were frozen with liquid nitrogen and stored for 6–9 months. In the laboratory of Dr. J. L. Pinckney (USC), excess water was removed and the filters for HPLC analysis were analyzed in the dark on a Shimadzu dual LC10-AT vp and Controller SCL-10 A vs binary gradient pump. Pigments on the filters were extracted after they were allowed to incubate for 18–24 h in an acetone solution. The supernatant separated from the filter was extracted and inserted into smaller amber vials. The HPLC analysis was run with solvent A of 80% methanol and 20% ammonium acetate and a solvent B of 80% methanol and 20% acetone. Spectra measurements between 380–700 nm were taken every 2 s and peaks were identified based on retention time. CHEMTAX, a matrix factorization program, was used to optimize the contribution of the selected groups to total Chl *a* (Mackey et al., 1996). The taxonomic groups, dinoflagellates (both gyroxanthin and peridinin types), chlorophytes, diatoms, cyanobacteria, cryptophytes, chrysophytes, and prymnesiophytes, were selected according to the "hierarchical guide to interpreting pigment data" (Wright and Jeffrey, 2006). Initial pigment ratios were selected from the literature and regional studies (Latasa et al., 2004; Latasa, 2007; Mackey et al., 1998; Ornolfsdottir et al., 2003; Redalje et al., 2008; Van Lenning et al., 2003; Zapata et al., 2004). The initial pigment ratio was optimized using multiple randomly generated starting points as seed values (Wright et al., 2009). Output ratios from the previous runs were used as input values for successive runs (Latasa, 2007). Values are reported here as absolute chlorophyll units.

A second CTD cast occurred at each station to collect near-bottom water (Grabowski, 2010). The contents of four or five 5 L Niskin bottles were poured through a 10 μm mesh net suspended on deck. Samples were also preserved with 4–5% borate-buffered formalin. In the laboratory approximately 2 ml collected from the bottom plate of the 100 ml settling column was rinsed with 3 ml of filtered seawater to ensure all organisms were collected from the settling slide. The 5 ml sample was then size fractionated through a 100 μm mesh and analyzed on a Fluid Imaging Flow Cytometer (FlowCAM). The FlowCAM was set up on auto image mode with the 100 μm flow cell and the 10x objective while pumping at an average setting of about 7 on fast mode. Size filters were applied to isolate and capture particles between 10–100 μm in equivalent spherical diameter (ESD). To ensure no contamination between samples the flow cell was cleaned thoroughly with filtered seawater and methanol between samples.

Between the pre-front and post-front surveys, sediment samples were collected at two stations: BA3 at 30 m isobath and BA5 near the 40 m isobath. Benthic $O_2$ and nutrient fluxes were measured during shipboard incubations (methods modified from Thomas and Blair, 2002; Thomas et al., 2002). Sediment for shipboard flux incubations was collected with a box corer after recording the texture and biological character of the sediment surface. After recovery of the box corer, a 14.5 cm-i.d. Lucite chamber was pushed into the sediment. The subcores were immediately removed from the box corer.

All shipboard incubations were conducted in both light and dark at bottom water temperatures (26 °C) and atmospheric pressure. Supernatants within each chamber were stirred continuously and monitored for $O_2$ and nutrient concentrations every 2 h for 8 h in the light and for 12 h in the dark. $O_2$ concentrations were measured using a modified micro-Winkler technique (Strickland and Parsons, 1972), which has a precision of $\pm 1\%$. $NO_3^- + NO_2^-$ and ammonium ($NH_4^+$) were determined colorimetrically at NCSU using an automated Quattro Continuous-Flow Analysis system (Grasshoff et al., 1983). Precision of the analysis was 0.3 μM for $NH_4^+$ and 0.1 μM for $NO_3^- + NO_2^-$. The detection limit for $NH_4^+$ was 0.5 μM and $NO_3^- + NO_2^-$ is 1.4 μM.

Sediment samples for porewater and porosity analyses were collected with a ship-supplied Oceanic Instruments MC-800 multi-corer (Barnett et al., 1984; Hopkinson et al., 2001). Porewater was extracted using sippers inserted into the sediment

from the side. Porewater was analyzed for $NO_3^- + NO_2^-$ and $NH_4^+$ concentrations at NCSU as described above. Porewater supported fluxes were calculated using Fick's first law:

$$J_{diff} = -\Phi D_s dC/dz$$

wherein $\Phi$ is the sediment porosity, $D_s$ is the sediment diffusion coefficient for the nutrient species corrected for tortuosity, $z$ is depth, and $dC/dz$ is the concentration gradient of the nutrient (Li and Gregory, 1974, Ullman and Aller, 1982). Sediment cores targeted for porosity measurements were extruded and sliced at 1 cm intervals to 3 cm and stored in 50 mL centrifuge tubes. Porosity samples were oven dried and weighed. Particle density of 2.7 g $cm^{-3}$ was used to calculate porosity.

## 3. Results

### 3.1. Cruise context during October 2008

PAR (Fig. 2) measured at the ANS (Fig. 1) generally decreased through October 2008. Oscillating air pressure and wind speed (Fig. 2) through October 2008 at NB 42039 (Fig. 1) were symptomatic of periodic cold fronts passing at ~6 d intervals. The resulting GUI (Fig. 3) for October 2008 during stronger wind events generally were downwelling favorable. In response to decreasing radiation and frequent cold front passage, surface water temperature decreased from 27.5 to 24.9 °C through the month and from 27.1° to 26.3 °C over the course of the cruise (Fig. 2). Based on the NB 42039 (Fig. 4), the pre-front wind speed

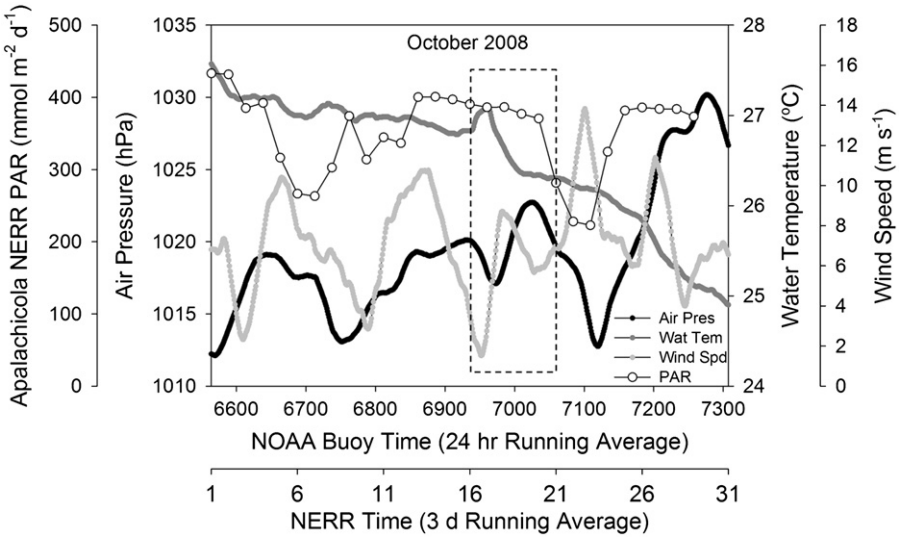


**Fig. 2.** Three day running average photosynthetically active radiation (PAR; mmol $m^{-2}$ $d^{-1}$) measured at ANS and 24 h running average air pressure (hPa), wind speed (m $s^{-1}$) and water temperature (°C) measured at NB 42039 between 1–31 October 2008. The 16–21 October cruise interval at the sample site is marked by the dashed line box.

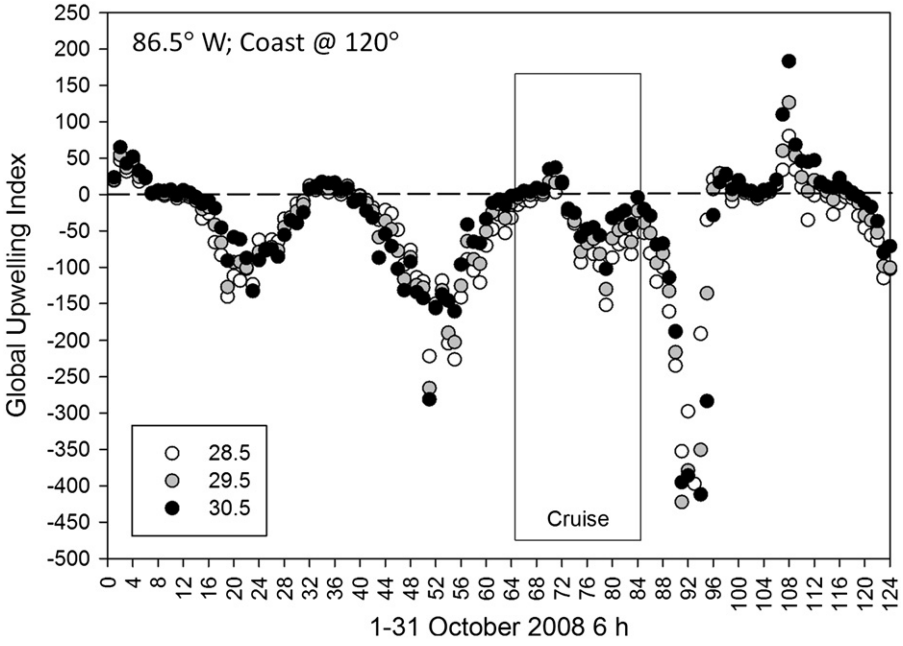


**Fig. 3.** Global Upwelling Index at 28.5°, 29.5° and 30.5°N calculated along 86°W with the coast at 120° clockwise from true north every 6 h from 16–21 October 2008. Upwelling (downwelling) is positive (negative).

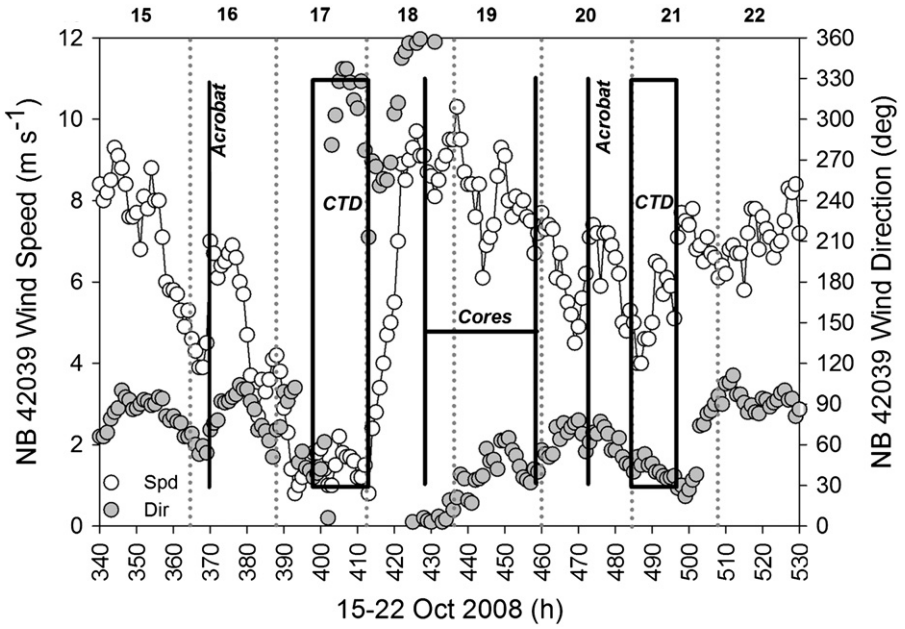


**Fig. 4.** One hour records of wind speed (m $s^{-1}$) and the direction (degrees from true north) from which the wind is blowing as measured at NB 42039 during the 15–22 October 2008 cruise interval. The times for Acrobat surveys, CTD stations and coring are marked.

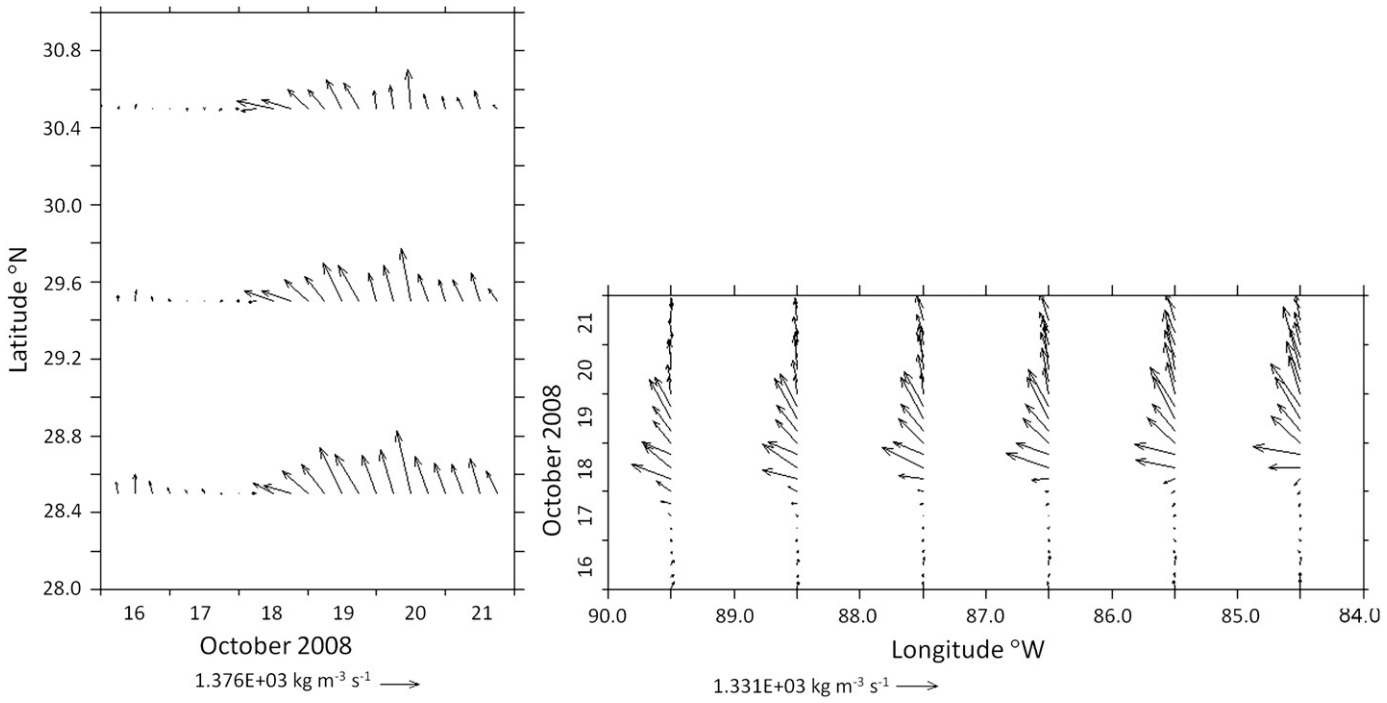


**Fig. 5.** Ekman transport vectors at the 86°W along 28.4°, 29.6° and 30.4°N and at 30°N along 84.5°, 85.4°, 86.5°, 87.5°, 88.5° and 89.5°W from 16–21 October 2008.

on 16 October 2008 was $<4$ m $s^{-1}$ from the E ($\sim$90°). Cold front influence began at 0100 GMT 18 October 2008 when wind speed increased to an average of $\sim$9 m $s^{-1}$ from the NW ($\sim$315°) for $\sim$24 h. The wind then turned to the NE gradually decreasing from 9 to 6 m $s^{-1}$ over the next 48 h. Post-front wind speed remained $\sim$7 m $s^{-1}$ generally from the E (90°). After 18 October 2008, Ekman transport vectors (Fig. 5) generally rotated northwest to north along 86°W between 28°N and the coast and along 30°N between 84–90°W in support of a relatively weak downwelling event (Fig. 3). The timing of the Acrobat and CTD surveys of the BA transect (Fig. 1) and of the coring effort at BA3 and BA5 (Fig. 1 insert gray box) considered next are marked on the NB 42039 wind record (Fig. 4).

### 3.2. Pre-front vs post-front acrobat

Acrobat cross-shelf sections provided a near-synoptic view (4–5 h duration) of surface to near-bottom (5–10 m off bottom inside the 40 m isobath and 10–20 m off bottom beyond the 40 m isobath) water column temperature (Fig. 6A, E), salinity (Fig. 6B, F), density (Fig. 6C, G) and oxygen saturation (Fig. 6D, H). Pre-front (Fig. 6A–D) during the 16 October 2008 transect (Fig. 4),

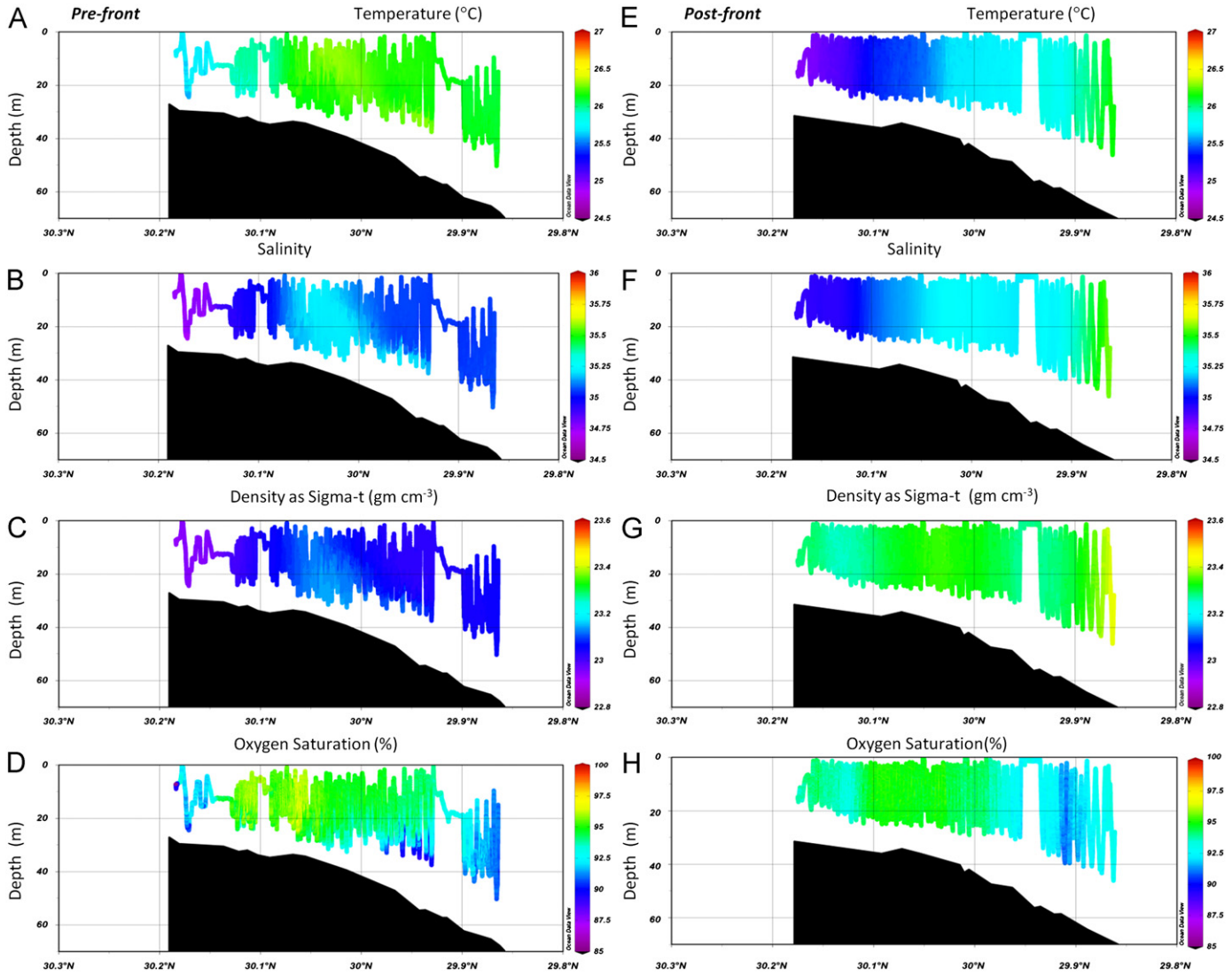


**Fig. 6.** Undulating Acrobat sections along transect for pre-front (left) and post-front (right) temperature (A, E; °C), salinity (B, F), potential density as sigma-*t* (C, G; kg m$^{-3}$) and oxygen saturation (D, H; %).

water inside the 35 m isobath at ~25.8 °C and 34.6 was relatively dense (22.8 kg m$^{-3}$) with ~92% oxygen saturation. Water between the 35–45 m isobaths was warmer (~26.4 °C), higher salinity (~35.2), higher density (~23.2 kg m$^{-3}$), and higher oxygen saturated (~96%) than inner shelf water. Cooler (~26 °C), lower salinity (~35), more dense (~23 kg m$^{-3}$), less oxygen saturated (~92%) water again occurred beyond the 45 m isobath. The density section (Fig. 6C) exhibited vertical stratification of the water column between the 35–55 m isobaths. Post-front (Fig. 6E–H) during the 20 October 2008 transect (Fig. 4), colder (~24.8 °C), lower salinity (~34.8), lower density (~23.2 kg m$^{-3}$) water inshore gradually graded to warmer (~26.2 °C), higher salinity (~35.7), higher density (~23.5 kg m$^{-3}$) water offshore. Oxygen saturation remained highest (~95%) between the 35–45 m contours, but the no vertical stratification was observed along transect.

Acrobat-derived, biologically related measurements included turbidity (Fig. 7A, E), total LOPC counts (Fig. 7B, F), chlorophyll (Fig. 7C, G) and CDOM (Fig. 7D, H). Pre-front, turbidity and total LOPC counts exhibited vertical structure that coincided with the vertical density stratification between the 35–55 m isobaths. Chlorophyll was more concentrated near-bottom but especially between the 35–40 m isobaths. CDOM exhibited a complicated pattern with highest values within the 30 m isobath and beyond the 60 m isobath and with the lowest values between the 35–40 m isobaths. Post-front, coherent vertical structure disappeared, but cross-shelf structure remained. Transect turbidity was highest between the 30–40 m and 50–60 m isobaths. Transect total LOPC count was lowest offshore of the 50 m isobath and was especially high in a band between the 35–40 m isobaths. Transect chlorophyll was highest between the 35–50 m isobaths. Transect CDOM was highest inshore of the 35 m contour and between the 50–60 m isobaths and lowest along the 35 m isobath and offshore of the 70 m isobath.

### 3.3. Pre-front vs post-front CTD

CTD profiles complemented the undulating Acrobat surveys with bottom (1 m off bottom) and surface (in the upper 1 m) samples. The pre-front CTD survey at eight stations required ~12 h to complete and was run mostly in daylight except inshore of the 25 m isobath. Water temperature (Fig. 8A) and salinity (Fig. 8B) exhibited vertical structure that resulted in density (Fig. 8C) stratification in most profiles (Fig. 8C). Water temperature, salinity and density generally increased toward the outer shelf. Calculated Brunt–Vaisala frequency (Fig. 9A, B) verified

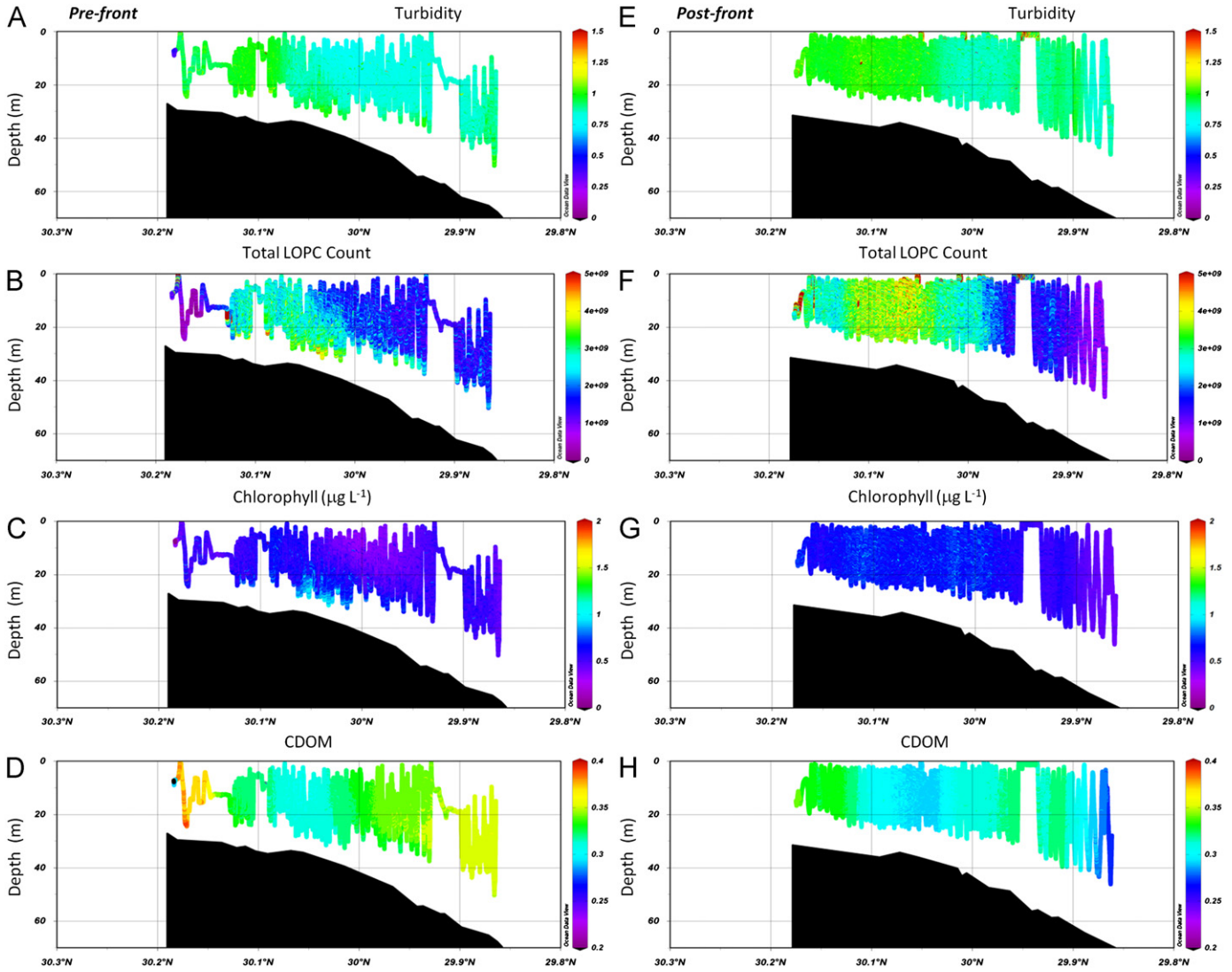


**Fig. 7.** Undulating Acrobat sections along transect for pre-front (left) and post-front (right) relative turbidity (A, E), total LOPC counts (B, F), chlorophyll (C, G; ug $L^{-1}$) and relative CDOM (D, H).

vertical stratification in all station profiles with values $>5$ cycles $h^{-1}$ in each profile. All profiles exhibited a minimum frequency at ~20 m depth. Potential PAR attenuation (Fig. 10A), based on water column transmissometry and thus independent of daylight showed that the euphotic zone extended to ~16 m across the shelf. Beam transmission (Fig. 10B) generally exceeded 75% throughout the water column to the 45 m isobath. Farther offshore, beam transmission was less than 70% below 45 m depth. $NO_3^- + NO_2^-$ concentrations (Fig. 10C) were generally ~2 μM inshore of the 25 m isobath, increased to ~5 μM near-surface and to ~4 μM near-bottom between the 30–40 m isobaths, decreased to ~2 μM between the 40–50 m isobaths, and increased to 6 μM below 50 m and to ~3 μM near-surface beyond the 55 m isobath.

The post-front CTD survey at nine stations required ~6.5 h to complete and was run mostly at night except offshore of the 40 m isobath. Both water temperature (Fig. 8D) and salinity (Fig. 8E) lacked vertical structure inside the 50 m isobath and increased toward the outer shelf. Density (Fig. 8F) was essentially constant out to the 40 m isobath, but then increased. Calculated Brunt–Vaisala frequency (Fig. 9C, D) verified the decreased vertical stratification in all station profiles post-front with values $>5$ cyles $h^{-1}$ only below 40 m depth. Potential PAR attenuation (Fig. 10D) based on water column transmissometry and thus independent of daylight showed that the euphotic zone extended to ~15 m across the shelf. Beam transmission (Fig. 10E) generally was $<72.5\%$ between 0–10 m depth and $>72.5\%$ below 10 m depth cross-shelf. The offshore mid-water column was clearer than the inshore mid-water column. Near-bottom beam transmission was below 65% beyond the 45 m isobath. $NO_3^- + NO_2^-$ concentrations (Fig. 10F) were ~1–2 μM across the shelf.

### 3.4. *Pre-front and post-front phytoplankton biomass and community composition*

Pre-front, continuous in-vivo relative fluorescence (Fig. 11A) profiles exhibited a maximum near-bottom at the 30 m isobath and higher values throughout the water column above the 40–50 m isobaths. HPLC-based chlorophyll *a* concentrations were $<0.3$ μg $L^{-1}$ near-surface above the 25–35 m isobaths and offshore below 15 m depth beyond the 55 m isobath (Fig. 11B), $>0.75$ near-bottom between the 20–30 m isobaths with a maximum of ~1.5 μg $L^{-1}$ at the 30 m isobath, and ~0.75 μg $L^{-1}$ throughout the water column between the 35–50 m isobaths (Fig. 11B). Based on HPLC/CHEMTAX, gyroxanthin-containing dinoflagellates occurred cross-shelf but dominated the water

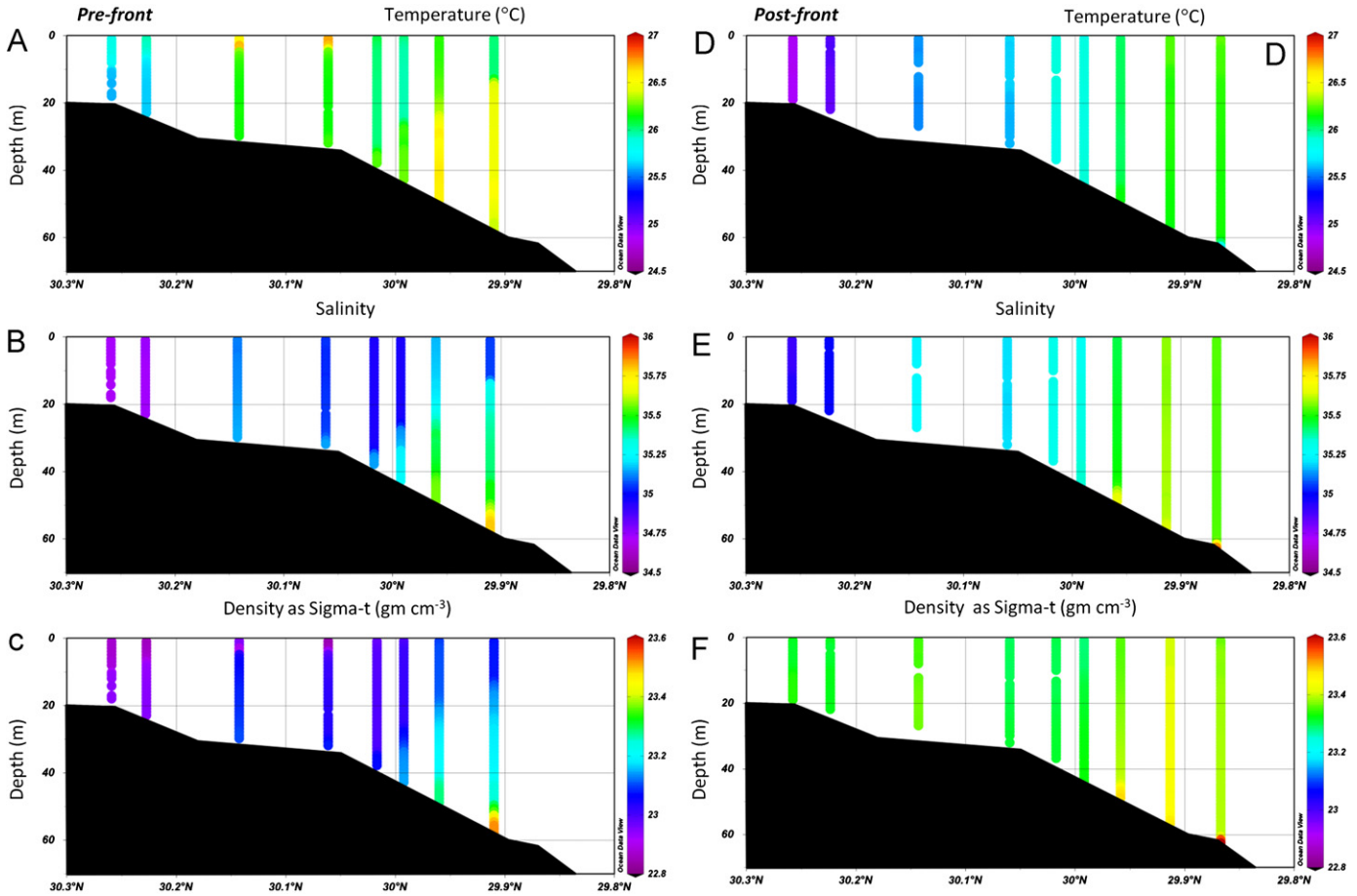


**Fig. 8.** CTD sections along transect for pre-front (left) and post-front (right) temperature (A, D; °C), salinity (B, E), and density as sigma-t (C, F; kg $m^{-3}$). Stations are marked by the vertical dots.

column when chlorophyll *a* exceeded 1 μg $L^{-1}$ (Fig. 12A) near-bottom at the 30 m isobath. Diatoms contributed significantly to the near-bottom chlorophyll *a* maximum at the 30 m isobath and also at the 50 m isobath (Fig. 12B). Chlorophytes (Fig. 12C) closely followed the diatom distribution. Prasinophytes (Fig. 13B) and cyanophytes (Fig. 13C) were highest at the surface above the 30–50 m isobaths. Cryptophytes (Fig. 13A) closely followed the diatom distribution near-bottom but also co-occurred with the prasinophytes and cyanophytes offshore. In agreement with HPLC, FlowCam analysis suggested that dinoflagellates were generally more abundant than diatoms and that pennate and centric diatoms were about equally abundant.

Post-front, continuous in-vivo relative fluorescence (Fig. 11C) was very low cross-shelf with a slight increase near-bottom within the 20 m isobath that extended from near-bottom at the 30 m isobath to the mid-water column offshore. HPLC-based chlorophyll *a* concentration was ~0.5 μg $L^{-1}$ above the 20 m isobath, ~0.7 μg $L^{-1}$ in the lower water column at the 35 m isobath, ~0.6 μg $L^{-1}$ in the upper water column at the 45 m isobath (Fig. 11D), and < 0.3 μg $L^{-1}$ near-surface on either side of the 45 m isobath (Fig. 11D). Based on HPLC/CHEMTAX, gyroxanthin-containing dinoflagellates (Fig. 12D) and diatoms (Fig. 12E) were reduced to chlorophyll *a* concentrations of ~0.2 μg $L^{-1}$ and contributed to the offshore chlorophyll *a* between the 35–60 m isobaths. Diatoms remained most abundant near-bottom between the 35–40 m isobaths. Cryptophytes (Fig. 13D), chlorophytes (Fig. 12F), and prasinophytes (Fig. 13E) also contributed to mid-shelf chlorophyll *a* with prasinophytes (Fig. 13E) increasing throughout the water column. Cyanophytes (Fig. 13F) moved inshore and increased in abundance across the shelf throughout the water column. In agreement with HPLC, FlowCam analysis suggested that phytoplankton abundance was reduced, but dinoflagellates retained a visible presence in the water column, and that pennate diatoms were now more abundant than centric diatoms.

### 3.5. Core samples

Sediments at the two corer stations were dominated by shell hash and coral rubble with quartz sands. The sediment fabric coarsened with core depth at BA 3 due to large shell fragments below 2 cm. Porosities were 50% at BA3 and 60% at BA5. The sediment surface at both stations was populated by burrows and tube linings and covered with fecal material from infauna.

Porewater $NO_3^- + NO_2^-$ concentrations in the 0–1 cm interval were 7.95 μM at BA3 (Fig. 1) and 1.47 μM at BA5 (Fig. 1). Porewater $NH_4^+$ concentrations in the 0–1 cm interval were 0 μM at BA 3 and 8.02 μM at BA5 and in the 2–3 cm interval were 11.29 μM at BA3. Near-nutrient concentrations above the sediment surface were higher at BA5 (2.71 μM $NO_3^- + NO_2^{-}{}^-$; 1.93 μM $NH_4^+$) than at BA3 (1.48 μM $NO_3^- + NO_2^-$; 1.93 μM $NH_4^+$). Porewater-supported $NO_3^- + NO_2^-$ fluxes were 0.55 μMoles $m^{-2}$ $h^{-1}$ at both stations (Table 1). Supported $NH_4^+$ fluxes were 0.28 μMoles $m^{-2}$ $h^{-1}$ at BA3 and 0.85 μMoles $m^{-2}$ $h^{-1}$ at BA5 (Table 1).

Diffusive fluxes measured in the chambers reflected the spatial heterogeneity of the sediments and its residents. Limited coring opportunities prevented additional replicate incubations ($n=2$ at BA3 and $n=3$ at BA5). Benthic oxygen demand (dark) was

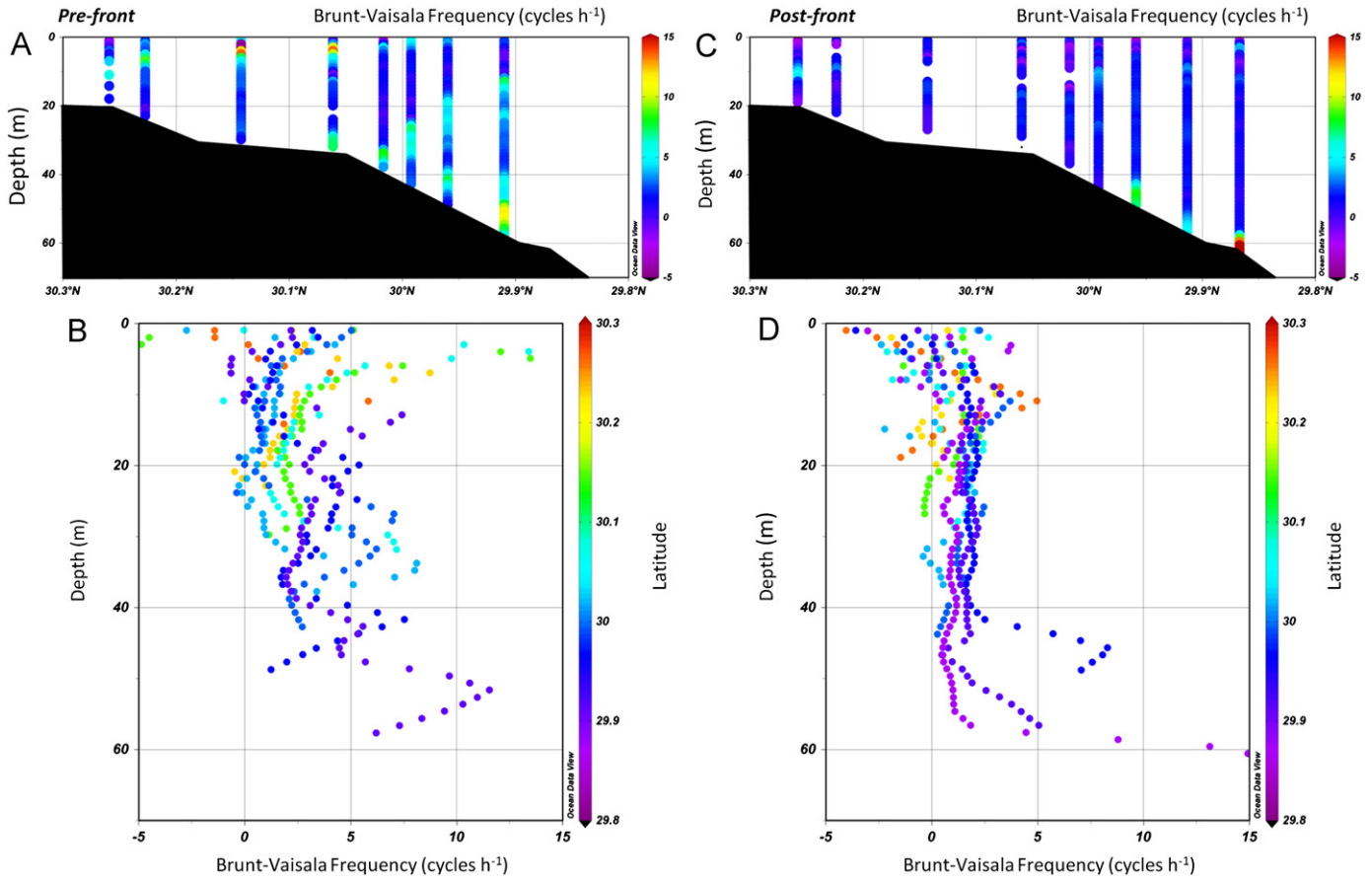


**Fig. 9.** CTD sections along transect for pre-front (left) and post-front (right) Brunt–Vaisala frequency (A, C; cycles $h^{-1}$). Stations are marked by the vertical dots. Vertical profiles for pre-front (left) and post-front (right) of Brunt–Vaisala frequency (B, D; cycles $h^{-1}$). Scale bar (B, D) represents station latitude.

$0.71 \pm 0.02$ mM $O_2$ $m^{-2}\,h^{-1}$ at BA3 and $0.35 \pm 0.12$ mM $O_2$ $m^{-2}\,h^{-1}$ at BA5. The sediment was a source of oxygen when incubated in the light. Fluxes measured in the light were $1.32 \pm 0.02$ mM $O_2$ $m^{-2}\,h^{-1}$ at BA3 and $1.71 \pm 0.41$ mM $O_2$ $m^{-2}\,h^{-1}$. $NO_3^- + NO_2^-$ fluxes were generally into the sediment and $NH_4^+$ fluxes were generally out of the sediment except at BA5 in the light (Table 1).

## 4. Discussion

The 15–21 October 2008 cruise occurred during the transition from summer (April to September) to winter (October to March) conditions on the FPS. October 2008 measurements for PAR from the ANS and for air pressure, wind speed and water temperature from NB 42039 showed that the cruise spanned a significant step in the forcing of the annual transition from vertically stratified to vertically well mixed on the FPS. NB 42039 measurements for 15–21 October 2008 highlighted the passage of a cold front during the cruise that provided ~30% of the sea surface temperature change during October 2008 at NB 42039. Since the trend of decreasing temperature continued through the rest of October 2008, both convection due to heat loss associated with decreasing incident radiation and colder air temperatures and energetic wind-driven vertical mixing likely contributed to the trend. The calculated Brunt–Vaisala frequencies confirmed the post-front development of a well mixed water column to 40 m depth.

The spatially intense and temporally synoptic Acrobat sections collected ~36 h before and toward the end of the frontal wind event provided a standard against which the comparatively sparse and more time consuming CTD/Rosette sections could be judged. Allowing for the temporal gap between samples, similar patterns observed for temperature, salinity and density with the two approaches supported the proposition that the CTD/Rosette stations for variables not measured by the Acrobat also provided a representative view of FPS patterns.

Shipboard survey results for 16–21 October 2008 on the FPS taken pre-front and post-front further documented a significant step in the cross-shelf transition from weak stratification to destratification suggested by the NB 42039 October 2008 record. To summarize, the pre-front vertical and cross-shelf structure associated with compensating water temperature and salinity patterns contributed to complex water mass patterns. Density increased to the 40 m isobath but decreased offshore. Phytoplankton growth conditions were set by a euphotic zone that extended to ~16 m depth and $NO_3^- + NO_2^-$ concentrations $> 3$ μM near-surface and near-bottom between the 30–40 m isobaths and offshore below 50 m depth. A near-bottom chlorophyll *a* maximum, typical of the summer condition on the FPS (McCulloch, 2011), existed between the 25–35 m isobaths composed of gyroxanthin-containing dinoflagellates, diatoms, cryptophytes and chlorophytes. A second chlorophyll *a* maximum, composed of cyanobacteria and low abundance haptophytes (not shown) in the upper half of the water column and of prasinophytes and low abundance gyroxanthin-containing and peridinin-containing dinoflagellates (not shown) throughout the water column, occurred above the 40–50 m isobaths where the near-surface low density plume ended. Post-front, the water

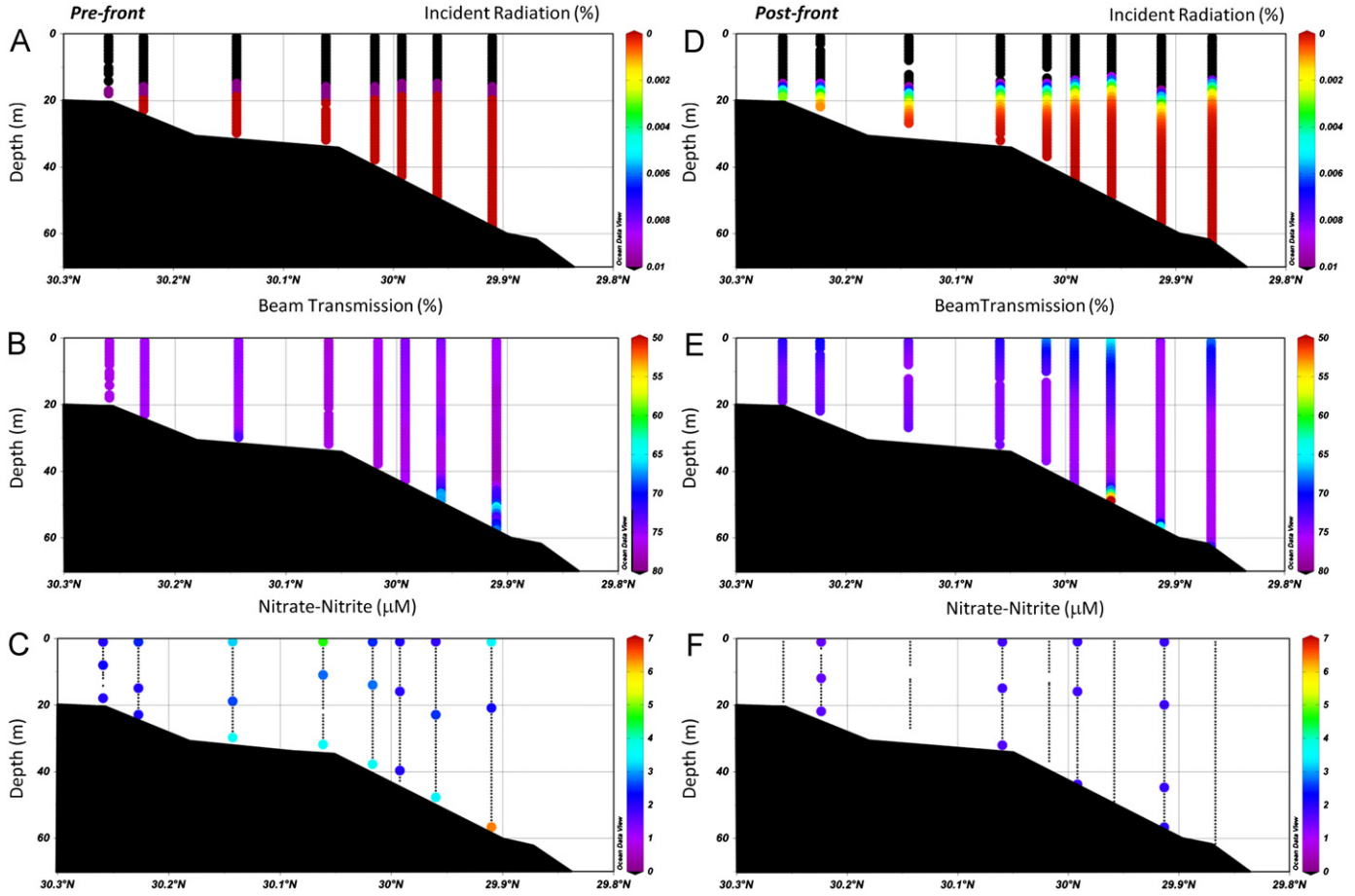


**Fig. 10.** CTD sections along transect for pre-front (left) and post-front (right) percent incident radiation (A, D; %), percent beam transmission (B, E, %), and nitrate-nitrite (C, F; μM). Stations are marked by the vertical dots.

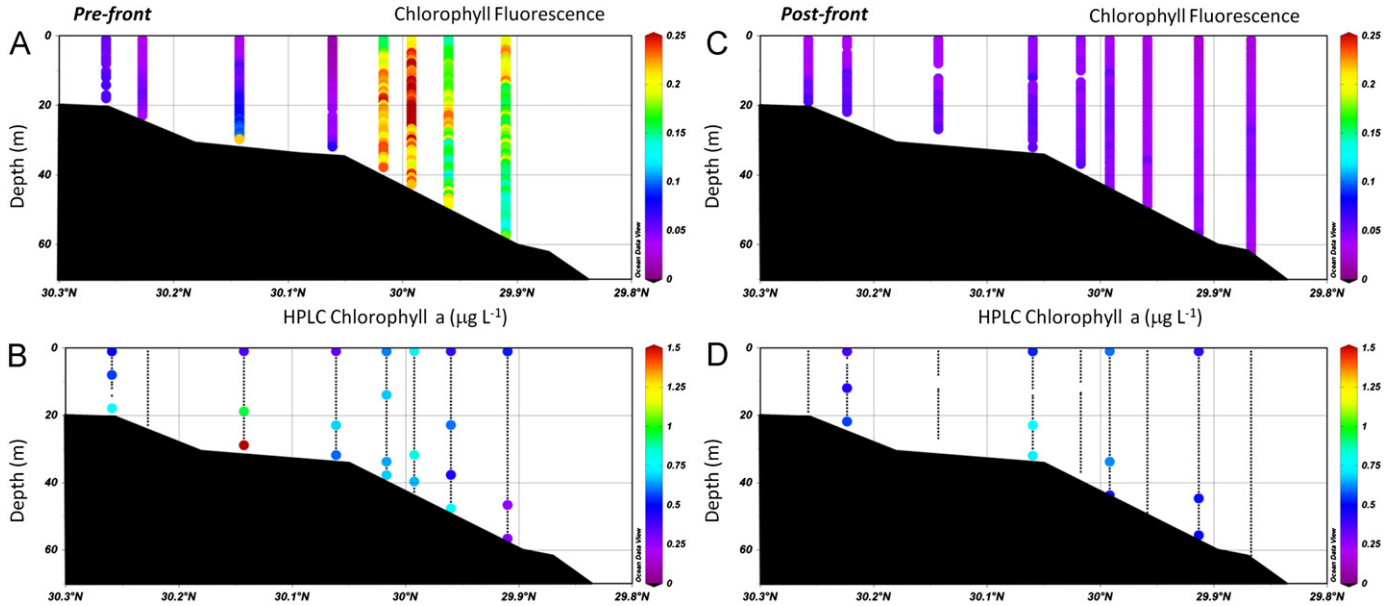


**Fig. 11.** CTD/rosette sections along transect for pre-front (left) and post-front (right) chlorophyll relative fluorescence (A, C) and HPLC chlorophyll *a* (B, D; μg $L^{-1}$). Stations are marked by the vertical dots.

column transitioned to destratification across the shelf with colder, lower salinity, lower density water inshore and warmer, higher salinity, higher density water offshore. Cross-shelf $NO_3^- + NO_2^-$ concentrations became more uniform at $<2$ μM, and the euphotic zone extended to $\sim$15 m depth. The pre-front near-bottom chlorophyll *a* maximum between the 25–35 m isobaths was reduced and contributed to a post-front offshore-directed plume composed of gyroxanthin-containing dinoflagellates and chlorophytes. Highest

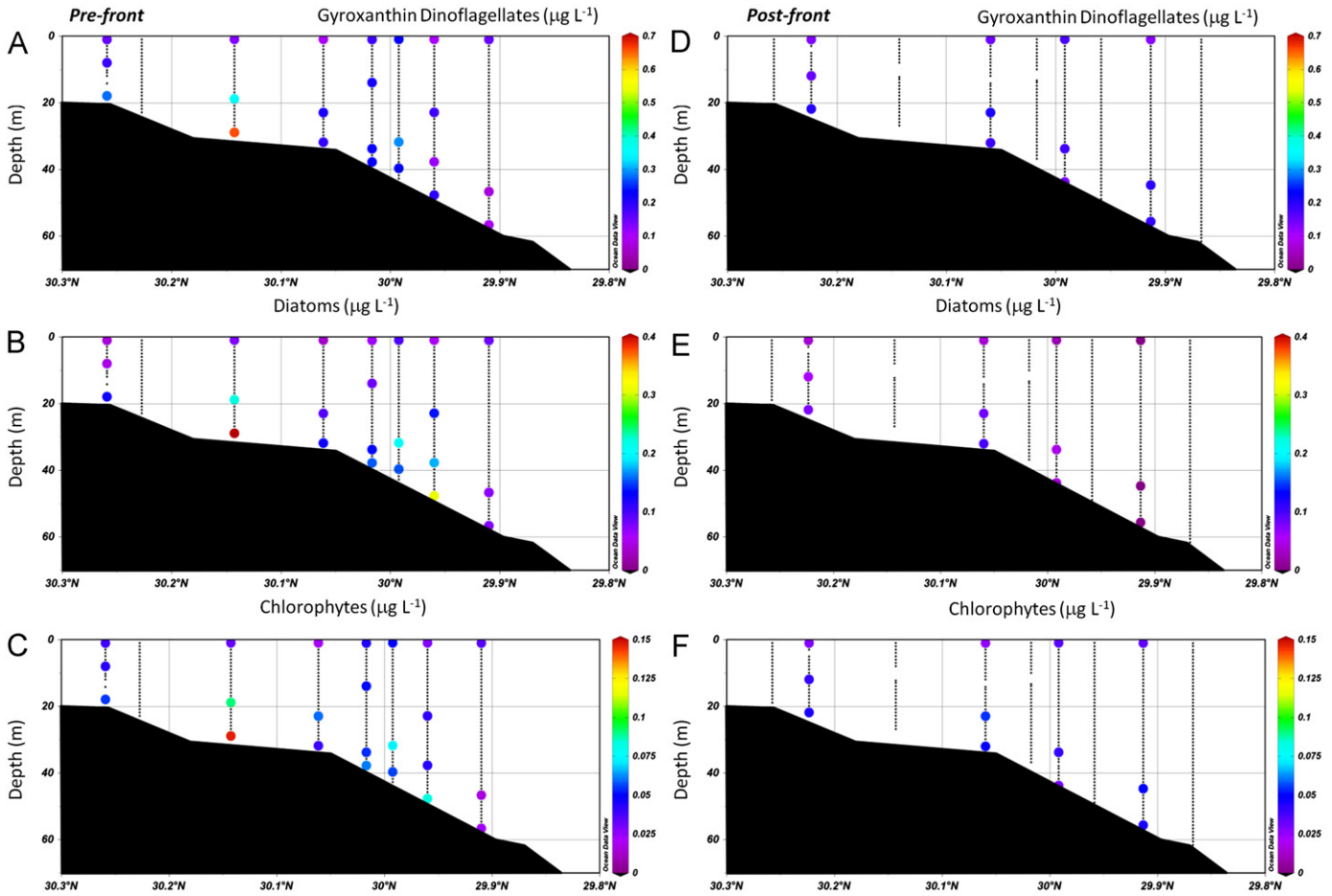


**Fig. 12.** CTD/rosette sections along transect for HPLC-derived chlorophyll *a* attributable to pre-front (left) and post-front (right) gyroxanthin-containing dinoflagellates (A, D; μg $L^{-1}$), diatoms (B, E; μg $L^{-1}$), and chlorophytes (C, F; μg $L^{-1}$).

cryptophytes abundance coincided with the prasinophyte and peridinin-containing dinoflagellate association. The second pre-front chlorophyll *a* maximum above the 40–50 m isobaths was enhanced as a result of cyanophytes increasing throughout the water column and the prasinophytes increasing in the lower half of the water column.

As the front passed, the water column was mixed to 40 m depth based on Brunt–Vaisala frequency, and upper water column flow initially occurred to the northwest and then to the north based on Ekman transport vectors. With a coastal angle of 120°, weak downwelling occurred on the FPS. As a first approximation, phytoplankton classes were considered passive tracers of the energetic conditions between the pre-front and post-front surveys. Rescaled gyroxanthin-containing dinoflagellate distributions (Fig. 14 A, C) showed that post-front cells were well mixed through the midshelf water column and moved offshore especially along the bottom, while rescaled cyanophyte distributions (Fig. 14 B, D) showed that the post-front cells were mixed through the water column cross-shelf and moved onshore at the surface. The cyanophyte connection with *K. brevis* (Walsh and Steidinger, 2001) was enhanced as a result of frontal passage.

Between 1985–2004, the greatest proportion of collected samples with $>100{,}000$ *K. brevis* cells $L^{-1}$ indicative of blooms occurred between July–December (http://myfwc.com/research/redtide/archive/historical-database/fl-red-tide-historical-database/). The only known gyroxanthin-containing dinoflagellates in the Gulf of Mexico are *K. brevis* and *Karenia mikimotoi* (Ornolfsdottir et al., 2003). Since gyroxanthin-containing dinoflagellates substantially contributed to the pre-front phytoplankton community, water column changes due to cold front passage have implications for *K. brevis* bloom initiation on the FPS. Representative of the July to 18 October part of the bloom season in 2008 (McCulloch, 2011), a large pre-front concentration of gyroxanthin-containing dinoflagellates occurred near-bottom between the 25–35 m isobaths with lower concentrations common throughout the mid-shelf water column (Fig. 9A). Representative of the 18 October to December part of the bloom season in 2008, the pre-front near-bottom cells were largely dispersed into the post-front water column but continued to exhibit, albeit reduced, near-bottom and near-surface maxima farther offshore (Fig. 11D). Coastal *K. brevis* blooms may be seeded by near-bottom populations under upwelling favorable winds (Janowitz and Kamykowski, 2006; Walsh et al., 2003; Janowitz et al., 2008; McCulloch, 2011) and by surface populations under downwelling favorable winds (Hetland and Campbell, 2007) with accumulation facilitated by behavioral trapping at coastal fronts under either condition (Janowitz and Kamykowski, 2006). On average, the GUI for 2008 (Fig. 15A) was predominantly weakly upwelling favorable from March through August and predominantly downwelling favorable the rest of the year. However, both upwelling and downwelling events occurred in all seasons (Fig. 15B) with greatest intensity and variability generally in the fall-winter except in response to tropical storms like Faye in August 2008.

The mechanisms contributing to the pre-front near-bottom chlorophyll *a* maximum between the 30 m isobaths with the 1% light level at 18 m is unclear. Diel vertical migration (Kamykowski et al., 1998) may have contributed to the aggregation of gyroxanthin-containing dinoflagellates. At maximum measured swimming speeds of $\sim$1.4 m $h^{-1}$ (McKay et al., 2006), *K. brevis* cells could migrate for 12 h from night depths of 30 m characterized

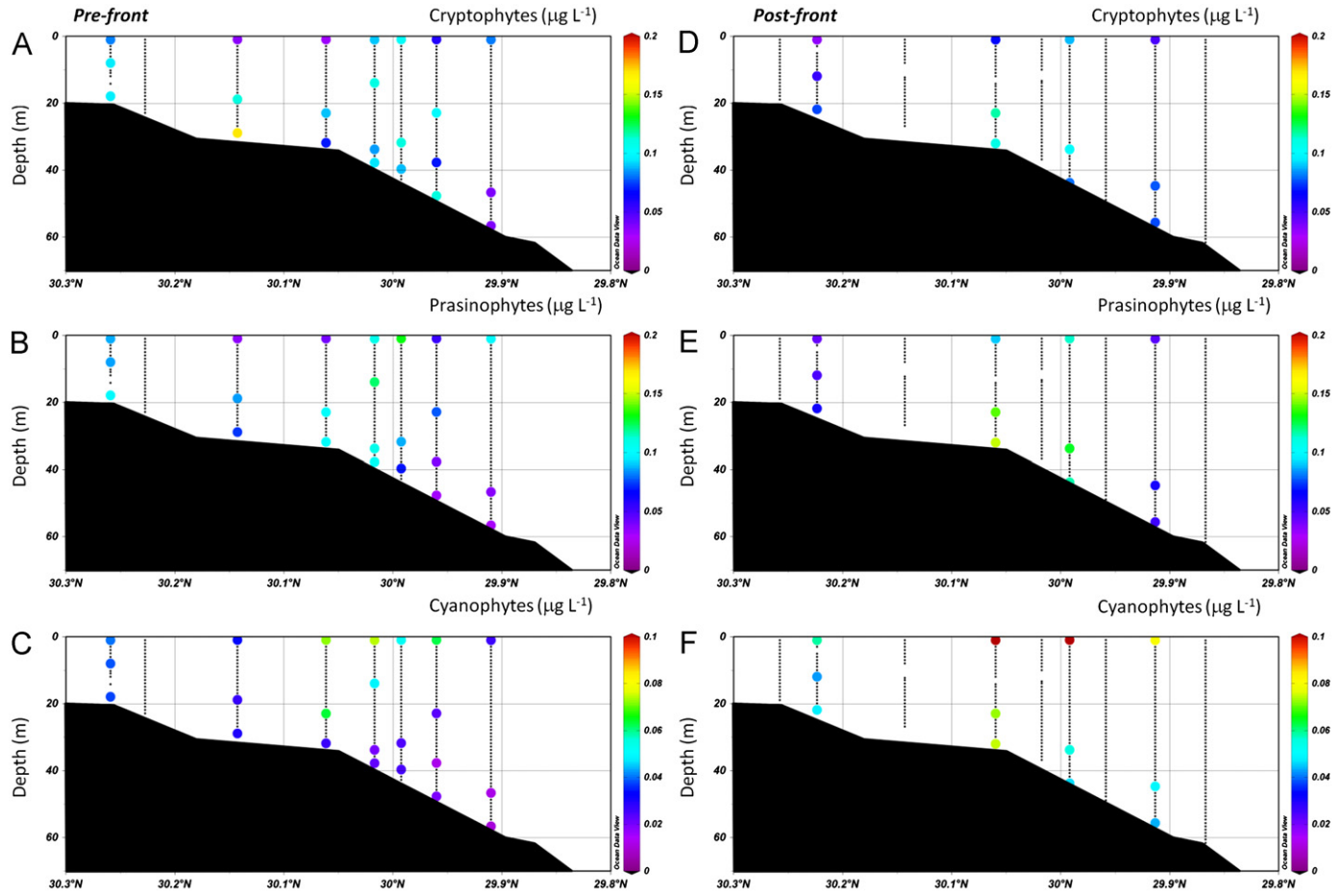


**Fig. 13.** CTD/rosette sections along transect for HPLC-derived chlorophyll *a* attributable to pre-front (left) and post-front (right) cryptophytes (A, D; μg $L^{-1}$), prasinophytes (B, E; μg $L^{-1}$), and cyanobacteria (C, F; μg $L^{-1}$).

**Table 1**
Benthic nutrient fluxes at Stations BA3 and BA5. Units are μMoles $m^{-2}$ $h^{-1}$. Negative fluxes indicate a flux into the sediment while a positive flux indicates a flux out of the sediment.

| | BA 3 ($n=2$) | BA 5 ($n=3$) |
|---|---|---|
| $NO_3^- + NO_2^-$ porewater-supported flux | 0.55 | 0.55 |
| $NO_3^- + NO_2^-$ chamber flux—dark | $-1.07 \pm 0.11$ | $-0.35 \pm 0.12$ |
| $NO_3^- + NO_2^-$ chamber flux—light | $-2.84 \pm 7.13$ | $1.71 \pm 0.41$ |
| $NH_4^+$ porewater-supported flux | 0.28 | 0.85 |
| $NH_4^+$ chamber flux—dark | $7.55 \pm 2.92$ | $6.02 \pm 4.19$ |
| $NH_4^+$ chamber flux—light | 3.40 | $-12.23 \pm 12.95$ |

by higher $NO_3 + NO_2$ to cover the 17 m distance needed to reach the lower euphotic zone (Fig. 14A). *K. brevis* cells may have utilized nutrients from the lower water column or directly from pore water (Sinclair, 2008; Sinclair and Kamykowski, 2008). The limited number of core replicates does not allow for establishment of clear sediment trends but, in general, these sediments are a potential source of nutrients to near-bottom populations of *K. brevis* and shell hash provides abundant pore space for *K. brevis* incursions. *K. brevis* descent to the sediment at night decreased competition with the benthic algae that clearly decreased the diffusive flux of nutrients across the sediment-water interface in light versus dark incubations. At the 30 m depth, *K. brevis* is able take up nitrate, ammonium and urea in the dark (Sinclair et al., 2006,2009) as required if the cells are near-bottom at night. A more pervasive ammonium flux from the sediment to the water column (Table 1) suggests ample reduced N-source for enhanced uptake by *K. brevis* over the diel cycle above the sediment interface at night and in low light (Sinclair et al., 2009). *K. brevis* therefore is theoretically capable of autotrophically maintaining a cell population under the pre-front conditions that existed on the FPS. On the other hand, *K. brevis* as a mixotroph utilized *Synechococcus* cells when grown under low light (Glibert et al., 2009). Whether *K. brevis* may utilize bacteria to maintain nutritional state well below the euphotic zone remains to be determined.

The diatoms, cryptophytes and chlorophytes also present in this chlorophyll *a* maximum can undertake diel vertical migrations (Moore and Villareal, 1996; Arvola et al., 1991; Richter et al., 2007), but for diatoms this is restricted to large cells, and the swimming capabilities of cryptophytes and chlorophytes generally are less ($<1$ m $h^{-1}$) than those of dinoflagellates. Since the PAR available to this chlorophyll *a* maximum was $<0.01\%$, these three phytoplankton groups may have been relict populations from a time when the euphotic zone was deeper.

Since zooplankton ingestion rates often hyperbolically increase with prey density (Hansen et al., 1997), the concentrated pre-front chlorophyll *a* maxima composed of gyroxanthin-containing dinoflagellates, diatoms, cryptophytes and chlorophytes between the 25–35 m isobaths may have facilitated macro-herbivore grazing compared to the more dispersed post-front chlorophyll *a* distribution. Though the presence of neurotoxic *K. brevis* may have modulated grazing, experimental studies concluded that selective grazing by co-occurring copepods simply lowered the rate of ingestion of *K. brevis* compared to more palatable species (Vargo, 2009). The near-bottom chlorophyll *a* maximum below the euphotic zone occurred in spite of probable grazing pressure from zooplankton that contributed to the

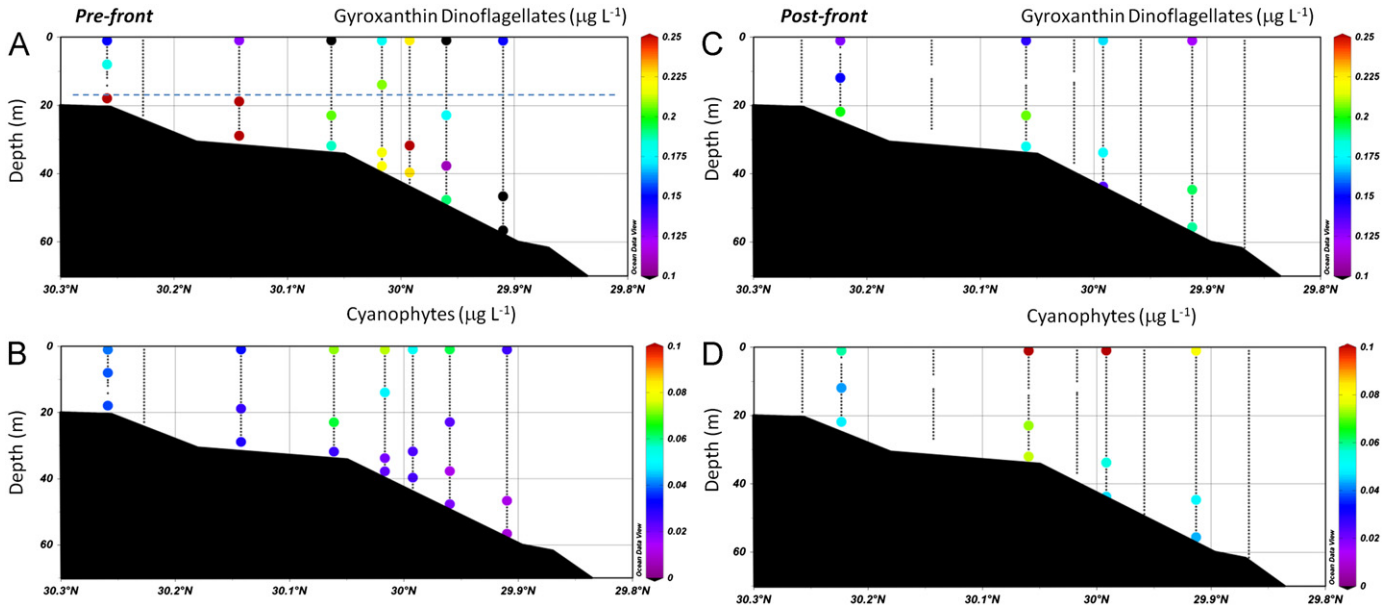


**Fig. 14.** CTD/rosette sections along transect for rescaled HPLC-derived chlorophyll *a* attributable to pre-front (left) and post-front (right) gyroxanthin-containing dinoflagellates (A, C; μg $L^{-1}$) and cyanophytes (B, D; μg $L^{-1}$).

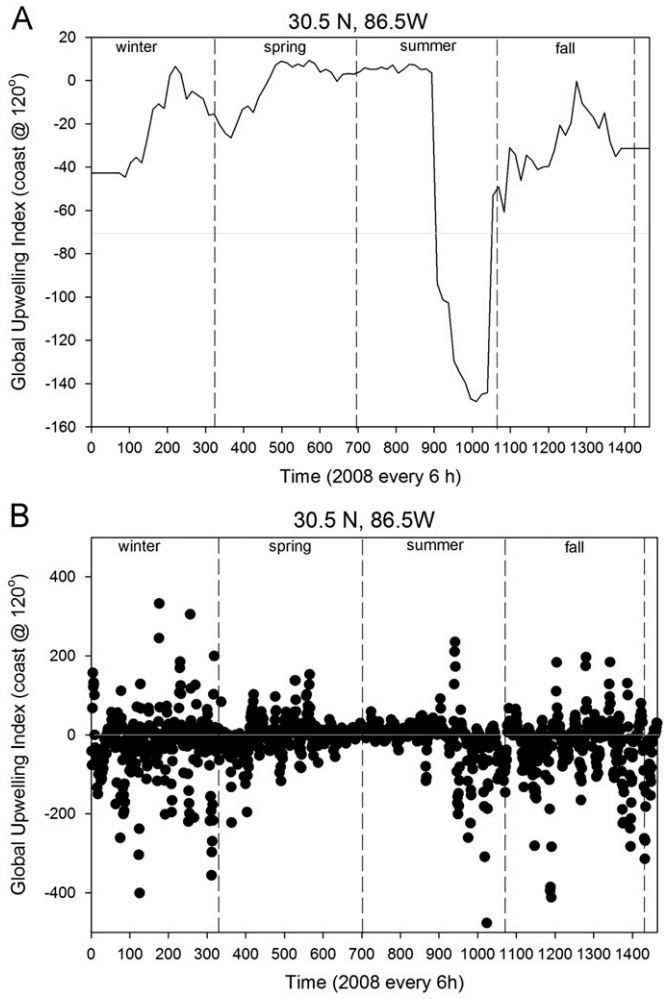


**Fig. 15.** Time series of the Global Upwelling Index for 1 Jan through 31 Dec 2008 from 30.5°N, 86.5°W for a coast angle of 120° as a running average (A) and as 6 hour raw data (B). Upwelling (downwelling) is positive (negative).

increased LOPC counts at the 30 m isobath and from an active infauna based on the observation that the sediment surface at both stations was populated by burrows and tube linings and covered with infaunal fecal material. Inferred grazing pressure further suggests that the pre-front phytoplankton distribution measured during the October 2008 cruise probably resulted from water column conditions that existed prior to the cruise and that the chlorophyll *a* maximum was probably waning, except possibly for *K. brevis*, under the measured conditions.

The snapshot views of the FPS before and after the passage of a cold front reported here demonstrate the dynamic changes that can occur cross-shelf in a short time interval. The changed patterns in multiple attributes provided useful comparisons, but essentially only two points in time were represented, and oceanic and along-shelf influences outside the sample domain were inadequately represented. Though the cruise provided a multivariate matrix that included physical, chemical and biological measurements, physical processes dominated the evolving patterns. Chemical and biological processes, operating at slower rates, lag physical redistribution and affect patterns only if more stable physical conditions allow (Cullen and Lewis, 1988). Improved spatial and temporal synopticity is needed to better define the context of FPS chemical and biological evolution.

## 5. Conclusions

Pre-front, FPS phytoplankton community structure was organized into inshore and offshore components. Gyroxanthin-containing dinoflagellates (i.e. *K. brevis*), though occurring cross-shelf, contributed significantly to the near-bottom chlorophyll maximum at the 30 m isobaths associated with elevated near-bottom nutrients in low light, while cyanophytes characterized offshore near-surface waters. Downwelling favorable winds during front passage moved the gyroxanthin-containing dinoflagellates offshore near-bottom and up in the water column, while the cyanophytes moved onshore near-surface. The observed step in the transition from the summer stratified condition to the winter destratified condition facilitated a change in the distribution

of *K. brevis* seed populations from a more concentrated, upwelling responsive, spring-summer near-bottom location to less concentrated fall-winter distribution throughout the water column equally responsive to upwelling or downwelling conditions and more generally co-occurring with cyanophytes.

## Acknowledgments

NSF grant OCE-0726271 awarded to Kamykowski/Janowitz/Thomas/Morrison supported the work. We thank the *R/V Pelican* crew and the LUMCON staff for their help and cooperation. PAR data were obtained from National Oceanographic and Atmospheric Association (NOAA), Office of Ocean and Coastal Resource Management, National Estuarine Research Reserve System-wide Monitoring Program, Centralized Data Management Office, Baruch Marine Field Lab, University of South Carolina (http://cdmo.baruch.sc.edu). Air pressure, wind speed and water temperature measured at NOAA Buoy (NB) 42039 (29.212°N 88.207°W) were obtained from U.S. Department of Commerce, NOAA, National Weather Service, National Data Buoy Center (http://www.ndbc.noaa.gov/). HPLC samples were run in the laboratory of Dr. J.L. Pinckney, University of South Carolina.

## References

Arvola, L., Ojala, A., Barbosa, F., Heaney, S.I., 1991. Migration behaviour of three cryptophytes in relation to environmental gradients: an experimental approach. European Journal of Phycology 26, 361–373.

Barnett, P.R.O., Watson, J., Connelley, D., 1984. A multiple corer for taking virtually undisturbed samples from shelf, bathyal and abyssal sediments. Oceanologica Acta 7, 399–408.

Chapman, D.C., Gawarkiewicz, G., 1993. On the establishment of the seasonal pycnocline in the middle Atlantic bight. Journal of Physical Oceanography 23, 2487–2492.

Cullen, J.J., Lewis, M.R., 1988. The kinetics of photoadaptation in the context of vertical mixing. Journal of Plankton Research 10, 1039–1063.

Glibert, P.M., Burkholder, J.M., Kana, T.M., Alexander, J., Skelton, H., Shilling, C., 2009. Grazing by *Karenia brevis* on *Synechococcus* enhances its growth rate and may help to sustain blooms. Aquatic Microbial Ecology 55, 17–30, http://dx.doi.org/10.3354/ame01279.

Grabowski, K.E., 2010. Near bottom dinoflagellate populations on the northwest Florida Shelf. MS Thesis. North Carolina State University.

Grasshoff, K., Ehrhardt, M., Kremling, K., 1983. Methods of seawater analysis, 2nd ed.. Verl.Chem., Weinheim, p. 419.

Hansen, P.J., Bjamsen, P.K., Hansen, B.W., 1997. Zooplankton grazing and growth: Scaling within the 2–2,000 μm body size range. Limnology and Oceanography 42, 687–704.

He, R., Weisberg, R.H., 2001. West florida shelf circulation and temperature budget for the 1999 spring transition. Continental Shelf Research 22, 719–748.

He, R., Weisberg, R.H., 2003. West Florida shelf circulation and temperature budget for the 1998 fall transition. Continental Shelf Research 23, 777–800.

Hetland, R.D., Campbell, L., 2007. Convergent blooms of *Karenia brevis* along the Texas coast. Geophysical Research Letters 34, L19604, http://dx.doi.org/10.1029/2007GL030474.

Hopkinson Jr., C.S., Giblin, A.E., Tucker, J., 2001. Benthic metabolism and nutrient regeneration on the continental shelf of Eastern Massachusetts, USA. Marine Ecology Progress Series 224, 1–19.

Janowitz, G.S., Kamykowski, D., 2006. Modeled *Karenia brevis* accumulation in the vicinity of a coastal nutrient front. Marine Ecology Progress Series 31, 49–59.

Janowitz, G.S., Kamykowski, D., Liu, G., 2008. A three dimensional wind and behaviorally driven population dynamics model for *Karenia brevis*. Continental Shelf Research 28, 177–188 (Special issue).

Jeffrey, S.W., Mantoura, R.F.C., Wright, S.W., 1997. Phytoplankton Pigments In Oceanography: Guidelines to Modern Methods. UNESCO, Paris.

Kamykowski, D., Milligan, E.J., Reed, R.E., 1998. Biochemical relationships with orientation of the autotrophic dinoflagellate, *Gymnodinium breve*, under nutrient replete conditions. Marine Ecology Progress Series 167, 105–117.

Latasa, M., Scharek, R., Le Gall, F., Guillou, L., 2004. Pigment suites and taxonomic groups in Prasinophyceae. Journal of Phycology 40 (6), 1149–1155.

Latasa, M., 2007. Improving estimations of phytoplankton class abundances using CHEMTAX. Marine Ecology Progress Series 329, 13–21.

Li, Y.-H., Gregory, S., 1974. Diffusion of ions in Sea Water and in deep-sea sediments. Geochimica et Cosmochimica Acta 38, 703–714.

Liu, Y., Weisberg, R.H., He, R., 2006. Sea surface temperature patterns on the West Florida shelf using growing hierarchical self-organizing maps. Journal of Atmospheric and Oceanic Technology 23, 325–338.

Mackey, M.D., Mackey, D.J., Higgins, H.W., Wright, S.W., 1996. CHEMTAX- A program for estimating class abundances from chemical markers: application to HPLC measurements of phytoplankton pigments. Marine Ecology Progress Series 144, 265–283.

Mackey, D.J., Higgins, H.W., Mackey, M.D., Holdsworth, D., 1998. Algal class abundances in the western equatorial Pacific: estimation from HPLC measurements of chloroplast pigments using CHEMTAX. Deep-Sea Research Part I 45 (9), 1441–1468.

McCulloch, A., 2011. A Spatio-Temporal Context for the Phytoplankton Community Patterns of the Galápagos Archipelago and the Northwest Florida Shelf. Ph.D. Thesis. North Carolina State University.

McKay, L., Kamykowski, D., Milligan, E., Schaeffer, B., Sinclair, G., 2006. Comparison of swimming speed and photophysiological responses to different external conditions among three *Karenia brevis* strains. Harmful Algae 5, 623–636.

Moore, J.K., Villareal, T.A., 1996. Size-ascent rate relationships in positively buoyant marine diatoms. Limnology and Oceanography 41, 1514–1520.

Morey, S.L., O'Brien, J.J., 2002. The spring transition from horizontal to vertical thermal stratification on a midlatitude continental shelf. Journal of Geophysical Research, 107, 3097, 10.1029/2001JC000826.

Muller-Karger, F.E., Vukovich, F., Leben, R., Nababan, B., Hu, C., Myhre, D., 2000. Remote sensing study of upwelling in the northeastern Gulf of Mexico and of the effects of Hurricanes Earl and Georges. Annual Report: Year 2. U.S. Department of the Interior, Minerals Management Service, La. OCS Study MMS 2000. Gulf of Mexico OCS Region, New Orleans, p. 42.

Nyadjro, E.S., 2009. Spatial and temporal dynamics of benthic chlorophyll formation on the northwest Florida continental shelf. MS Thesis. University of North Carolina, Wilmington.

O'Dell, J.W., 1993. Method 353.2 Determination of Nitrate-Nitrite Nitrogen by Automated Colorimetry. Environmental Monitoring Systems Laboratory, Office of Research and Development, Environmental Protection Agency.

Ornolfsdottir, E.B., Pinckney, J.L., Tester, P.A., 2003. Quantification of the relative abundance of the toxic dinoflagellate, *Karenia brevis* (Dinophyta), using unique photopigments. Journal of Phycology 39 (2), 449–457.

Redalje, D.G., Lohrenz, S.E., Natter, M.J., Tuel, M.D., Kirkpatrick, G.J., Millie, D.F., Fahnenstiel, G.L., Van Dolah, F.M., 2008. The growth dynamics of Karenia brevis within discrete blooms on the West Florida shelf. Continental Shelf Research 28 (1), 24–44.

Richter, P.R., Hader, D.-P., Goncalves, R.J., Marcoval, M.A., Villafane, V.E., Helbling, E.W., 2007. Vertical migration and motility responses in three marine phytoplankton species exposed to solar radiation. Photochemistry and Photobiology 83, 810–817.

Sinclair, G.A., 2008. Physical and chemical constraints on the near-bottom ecology of *Karenia brevis*. Ph.D. Thesis. Marine, Earth and Atmospheric Sciences. North Carolina State University, Raleigh, NC.

Sinclair, G.A., Kamykowski, D., Milligan, E., Schaeffer, B., 2006. Nitrate uptake by *Karenia brevis*. I. Influences of prior environmental exposure and biochemical state on diel uptake of nitrate. Marine Ecology Progress Series 328, 117–124.

Sinclair, G.A., Kamykowski, D., 2008. Benthic-pelagic coupling in sediment associated populations of *Karenia brevis*. Journal of Plankton Research 30, 829–838.

Sinclair, G., Kamykowski, D., Glibert, P.M., 2009. Growth, uptake and assimilation of ammonium, nitrate, and urea, by three strains of *Karenia brevis* grown under low light. Harmful Algae 8, 770–780.

Smith, S.R., Jacobs, G.A., 2005. Seasonal circulation fields in the northern Gulf of Mexico calculated by assimilating current meter, shipboard ADCP, and drifter data simultaneously with the shallow water equations. Continental Shelf Research 25, 157–183.

Strickland, J.D.H., Parsons, T.R., 1972. A practical handbook of sea-water analysis, 2nd ed. Bulletin of the Fisheries Research Board of Canada, p. 167.

Thomas, C.J., Blair, N.E., 2002. Transport and alteration of uniformly $^{13}$C-labeled diatoms in mudflat sediments. Journal of Marine Research 60, 517–535.

Thomas, C.J., Blair, N.E., Alperin, M.J., DeMaster, D.J., Jahnke, R.A., Martens, C.S., Mayer, L., 2002. Organic carbon deposition on the North Carolina continental slope off Cape Hatteras (USA). Deep Sea Research Part II 49, 4687–4709.

Ullman, W.J., Aller, R.C., 1982. Diffusion coefficients in nearshore marine sediments. Limnology and Oceanography 27, 552–556.

Van Lenning, K., Latasa, M., Estrada, M., Saez, A.G., Medlin, L., Probert, I., Veron, B., Young, J., 2003. Pigment signatures and phylogenetic relationships of the pavlovophyceae (Haptophyta). Journal of Phycology 39 (2), 379–389.

Vargo, G.A., 2009. A brief summary of the physiology and ecology of *Karenia brevis* Davis (G. Hansen and Moestrup comb. nov.) red tides on the West Florida shelf and of hypotheses posed for their initiation, growth, maintenance, and termination. Harmful Algae 8, 573–584.

Walsh, J.J., Steidinger, K.A., 2001. Saharan dust and Florida red tides: the cyanophyte connection. Journal of Geophysical Research 106, 11597–11612.

Walsh, J.J., Weisberg, R.H., Dieterle, D.A., He, R., Darrow, B.P., Jolliff, J.K., Lester, K.M., Vargo, G.A., Kirkpatrick, G.J., Fanning, K.A., Sutton, T.T., Jochens, A.E., Biggs, D.C., Nababan, B., Hu, C., Muller-Karger, F.E., 2003. Phytoplankton response to intrusions of slope water on the West Florida shelf: models and observations. Journal of Geophysical Research 108, 3190, http://dx.doi.org/10.1029/2002JC001406.

Wang, D., Oey, L., Ezer, T., Hamilton, P., 2003. Near-surface currents in DeSoto Canyon (1997–99): comparison of current meters, satellite observation, and model simulation. Journal of Physical Oceanography 33 (1), 313–326.

Weisberg, R.H., Black, B.D., Yang, H., 1996. Seasonal modulation of the west Florida continental shelf circulation. Geophysical Research Letters 23, 2247–2250.

Weisberg, R.H., Black, B.D., Li, Z., 2000. An upwelling case study on Florida's west coast. Journal of Geophysical Research 105 (C5), 11459–11469.
Wright, S., Jeffrey, S., 2006. Pigment markers for phytoplankton production. In: Volkman, J. (Ed.), Handbook for Environmental Chemistry. Springer-Verlag, Berlin, pp. 71–104.
Wright, S.W., Ishikawa, A., Marchant, H.J., Davidson, A.T., van den Enden, R.L., Nash, G.V., 2009. Composition and significance of picophytoplankton in Antarctic waters. Polar Biology 32 (5), 797–808.
Yang, H., Weisberg, R.H., 1999. Response of the West Florida shelf circulation to climatological wind stress forcing. Journal of Geophysical Research 104 (C3), 5301–5320.
Zapata, M., Jeffrey, S.W., Wright, S.W., Rodriguez, F., Garrido, J.L., Clementson, L., 2004. Photosynthetic pigments in 37 species (65 strains) of *Haptophyta*: implications for oceanography and chemotaxonomy. Marine Ecology Progress Series 270, 83–102.